

# Quantifying strategies to minimize aerosol dispersion in dental clinics

Shamudra Dey<sup>1</sup>, Maryam Tunio<sup>2</sup>, Louis C. Boryc<sup>2</sup>, Brian D. Hodgson<sup>2</sup>, Guilherme J. M. Garcia<sup>1</sup> (✉)

1. Joint Department of Biomedical Engineering, Marquette University, Medical College of Wisconsin, Milwaukee 53226, USA

2. School of Dentistry, Marquette University, Milwaukee 53233, USA

## Abstract

Many dental procedures are aerosol-generating and pose a risk for the spread of airborne diseases, including COVID-19. Several aerosol mitigation strategies are available to reduce aerosol dispersion in dental clinics, such as increasing room ventilation and using extra-oral suction devices and high-efficiency particulate air (HEPA) filtration units. However, many questions remain unanswered, including what the optimal device flow rate is and how long after a patient exits the room it is safe to start treatment of the next patient. This study used computational fluid dynamics (CFD) to quantify the effectiveness of room ventilation, an HEPA filtration unit, and two extra-oral suction devices to reduce aerosols in a dental clinic. Aerosol concentration was quantified as the particulate matter under 10  $\mu\text{m}$  ( $\text{PM}_{10}$ ) using the particle size distribution generated during dental drilling. The simulations considered a 15 min procedure followed by a 30 min resting period. The efficiency of aerosol mitigation strategies was quantified by the scrubbing time, defined as the amount of time required to remove 95% of the aerosol released during the dental procedure. When no aerosol mitigation strategy was applied,  $\text{PM}_{10}$  reached 30  $\mu\text{g}/\text{m}^3$  after 15 min of dental drilling, and then declined gradually to 0.2  $\mu\text{g}/\text{m}^3$  at the end of the resting period. The scrubbing time decreased from 20 to 5 min when the room ventilation increased from 6.3 to 18 air changes per hour (ACH), and decreased from 10 to 1 min when the flow rate of the HEPA filtration unit increased from 8 to 20 ACH. The CFD simulations also predicted that the extra-oral suction devices would capture 100% of the particles emanating from the patient's mouth for device flow rates above 400 L/min. In summary, this study demonstrates that aerosol mitigation strategies can effectively reduce aerosol concentrations in dental clinics, which is expected to reduce the risk of spreading COVID-19 and other airborne diseases.

## Keywords

dental aerosols  
COVID-19  
extra-oral suction device  
high-efficiency particulate air (HEPA) filtration unit  
fallow time  
computational fluid dynamics (CFD) simulation

## Article History

Received: 23 August 2022

Revised: 12 November 2022

Accepted: 25 December 2022

## Research Article

© Tsinghua University Press 2022

## 1 Introduction

Many dental procedures are aerosol-generating and pose a risk for the spread of airborne diseases, including COVID-19, influenza, measles, tuberculosis, legionnaires disease, and SARS (Harrel and Molinari, 2004). Dental aerosols are generated by mechanical instrumentation used in a range of dental procedures, including drilling (e.g., high-speed handpiece, low-speed handpiece), polishing (e.g., air polisher, rotatory polisher), and cleaning (e.g., ultrasonic scaling, three-way syringe). Dental aerosols are composed of a mixture of water, saliva, blood, tooth debris, and dental

products. Research studies have illustrated the risk of disease transmission by demonstrating a higher aerosol concentration and a higher microbial concentration in air during dental procedures (Timmerman et al., 2004; Sotiriou et al., 2008; Pasquarella et al., 2012), and that bacterial contamination can be detected as far as 11 m away from the dental chair where the dental procedure was performed (Grenier, 1995).

The terms “aerosol” and “splatter” are used in the dental literature to distinguish particles of different sizes (Leggat and Kedjarune, 2001; Harrel and Molinari, 2004). The term “splatter” is used for droplets larger than about 10  $\mu\text{m}$  that

✉ ggarcia@mcw.edu

## Nomenclature

$d$	particle diameter ( $\mu\text{m}$ )	$(N_T)_{\text{EXP}}$	total number of particles released per second in dental procedure
$f_d$	fraction of particles in polydisperse distribution that have diameter $d$	$N_{\text{rp}}$	number of release points
$k_1$	rescaling factor	$N_{\text{added}}^d$	number of particles of diameter $d$ released per second
$m_d$	mass of one spherical particle of diameter $d$ ( $\mu\text{g}$ )	$N_{\text{removed}}^d$	number of particles of diameter $d$ that deposit or exit the fluid domain per second
$M_d(t)$	total mass of particles of diameter $d$ that remain airborne at time $t$ ( $\mu\text{g}$ )	$\text{PM}_{10}$	total concentration of particles in air with diameter under $10 \mu\text{m}$ ( $\mu\text{g}/\text{m}^3$ )
$N_d(t)$	number of particles of diameter $d$ that remain airborne at time $t$	$(\text{PM}_{10})_{\text{CFD}}$	particle concentration predicted by CFD before rescaling ( $\mu\text{g}/\text{m}^3$ )
$(N_d)_{\text{CFD}}(t)$	number of particles of diameter $d$ that remain airborne at time $t$ in CFD simulation	$(\text{PM}_{10})_{\text{EXP}}$	particle concentration observed experimentally ( $\mu\text{g}/\text{m}^3$ )
$(N_d)_{\text{EXP}}(t)$	number of particles of diameter $d$ that remain airborne at time $t$ in dental procedure	$t$	time (min)
$(N_d^0)_{\text{CFD}}$	number of particles of diameter $d$ released per second in CFD simulation	$V$	volume of air in dental clinic ( $\text{m}^3$ )
$(N_d^0)_{\text{EXP}}$	number of particles of diameter $d$ released per second in dental procedure	$\bar{v}$	volume-averaged air velocity (m/s)
$(N_T)_{\text{CFD}}$	total number of particles released per second in CFD simulation	$\rho$	particle density ( $\text{kg}/\text{m}^3$ )

deposit near the patient's mouth due to gravitational settling. The term "aerosol" is used for particles smaller than about  $10 \mu\text{m}$  that can stay airborne for an extended period of time. Both splatter and aerosols represent a risk to transmit infections, but aerosols are invisible to the naked eye and have the greatest potential of disease transmission to people more than six feet away from the infected patient (Harrel and Molinari, 2004; Klompas et al., 2020; Kumar and Subramanian, 2020).

Many studies have demonstrated that aerosol concentration increases in dental clinics during patient procedures (Grenier, 1995; Sotiriou et al., 2008; Pasquarella et al., 2012; Polednik, 2021; Dudding et al., 2022). Since the coronavirus that causes COVID-19 is found in saliva (To et al., 2020), dental healthcare workers are at an increased risk of contracting COVID-19. However, it remains unclear if the high aerosol levels in dental clinics are associated with a higher incidence of COVID-19 among dental healthcare workers. One study analyzed data from the United States Department of Labor and reported that dental healthcare workers have the highest occupational risk of contracting COVID-19 among different professions (Zhang, 2021). In contrast, a survey of dental healthcare workers in France reported that the prevalence of laboratory-confirmed COVID-19 among dentists was similar to the general population (Jungo et al., 2021). Furthermore, a study from Israel reported that the incidence of COVID-19 among

dental healthcare workers was lower than in the general population (Natapov et al., 2021). Thus, the available evidence suggests that in most cases standard infection control measures are effective at reducing the risk of transmission of airborne pathogens in dental clinics (Petti, 2016; Meethil et al., 2021).

While transmission of airborne pathogens in dental clinics is rare, some reported cases illustrate the risk. One documented case of disease transmission occurred in a medical office where the measles virus was spread through the ventilation system to multiple people (Harrel and Molinari, 2004). The source patient was a 12-year-old boy who was coughing. Of the seven people who acquired measles at this clinic, one entered the office one hour after the source patient had left. Another example that illustrates the risk of disease transmission by airborne pathogens comes from the SARS outbreak in China. An outbreak in a Hong Kong apartment complex was likely facilitated by the ventilation system spreading the SARS coronavirus between different apartment units (Harrel and Molinari, 2004).

Several strategies are used to minimize the risk of infection in dental clinics. Dental healthcare workers use personal protective equipment (PPE), such as gloves, gowns, and N-95 masks, to protect themselves. However, aerosols that remain suspended in air for an extended period of time represent a risk of contamination to consecutive patients treated at the same clinic and to clerical staff at the

reception desk who often do not wear protective masks. The gold-standard strategy to reduce aerosols in dental clinics is the use of a high-volume evacuator (HVE), which has been shown to reduce the contamination arising from the operative site by more than 90% (Harrel and Molinari, 2004). However, HVE utilization requires a human assistant (“four-handed dentistry”). This is a limitation because many treatments are performed by dental hygienists without an assistant. Another strategy to minimize aerosol dispersion is the rubber dam, which virtually eliminates contamination with saliva, reducing the source of contamination to the tooth being treated. However, it is not feasible to use the rubber dam in many dental procedures, such as routine prophylaxis, periodontal surgery, and subgingival restoration (Harrel and Molinari, 2004). Strategies such as the HVE, rubber dam, and saliva ejector are aimed at preventing aerosols from escaping from the patient’s mouth. Another category of aerosol mitigation strategies are engineering controls, which are aimed at capturing the aerosols after they have been released from the patient’s mouth. Engineering controls include increasing the ventilation rate of the dental clinic, using portable high-efficiency particulate air (HEPA) filtration units, and using extra-oral suction devices (also known as local exhaust ventilation). However, these engineering controls have not been universally adopted yet, in part because their effectiveness is poorly characterized.

One major question that dentists faced during the COVID-19 pandemic was when it was safe for a new patient to enter a room after the treatment of the previous patient. Research studies suggest that pathogens can remain airborne for at least 20 min after the dental treatment is completed (Chuang et al., 2014). Another major question is the determination of the optimal flow rate of HEPA filtration units and extra-oral suction devices. Higher flow rates are more effective at scrubbing aerosols, but higher flow rates also generate louder noises that can be a nuisance for patients and dental healthcare workers. Currently, it is difficult to predict the optimal flow rate that is effective at removing aerosols while minimizing noise. In this study, we apply computational fluid dynamics (CFD) to compare the aerosol removal efficiency of four engineering controls, namely (1) increasing room ventilation, (2) a portable HEPA filtration unit, (3) a circular extra-oral suction device, and (4) an elliptical extra-oral suction device. The CFD simulations are designed to represent 15 min of dental drilling followed by 30 min of a resting period. We estimate the minimal flow rate required to remove all particles emanating from the patient’s mouth using extra-oral suction devices. We also estimate the amount of time required for aerosol concentration to return to background levels as a function of the room ventilation and the HEPA filtration unit flow rate.

## 2 Methods

### 2.1 Geometry and flow rates

The dimensions of the dental clinic (height = 2.86 m, width = 3.31 m, depth = 3.58 m, volume = 33.9 m<sup>3</sup>) in this study are based on a single-chair dental clinic at the School of Dentistry at Marquette University. A 3D reconstruction of a human head was positioned on the dental chair (Fig. 1). We investigated the aerosol removal efficiency of three devices, namely two extra-oral suction devices and a portable HEPA filtration unit. The geometries of the two extra-oral suction devices were inspired by the Treedental dental suction unit (model TR-YP606D4, TREE USA Inc., Valley Cottage, NY, USA) and the Xuction HVE Dental Aerosol Reducer (Xuction Dental, Midlothian, VA, USA), respectively. The extra-oral suction device #1 had a circular inlet (diameter = 10 cm) positioned lateral to the patient’s mouth (Fig. 1(B)). The extra-oral suction device #2 had an elliptical inlet (major axis diameter = 42.5 mm, minor axis diameter = 12.5 mm, area = 417 mm<sup>2</sup>) positioned inferior to the patient’s mouth (Fig. 1(C)). The portable HEPA filtration unit was located at the corner of the room (Figs. 1(A) and 1(D)). It pulls air from its side and returns the filtered air through its top. Its dimensions and flow rates are based on the JADE air purification system (model SCA5000C, Surgically Clean Air, Toronto, Ontario, Canada). The geometry of the inlet vent on the ceiling was developed by Komperda et al. (2021) and kindly shared with us for this study.

The dental clinic has a ventilation of 3540 L/min (corresponding to 6.3 ACH (air changes per hour)) through inlet and outlet vents on the ceiling (Fig. 1). This ventilation rate was used in all simulations with the extra-oral suction devices and the HEPA filtration unit. To investigate the effect of increasing room ventilation, simulations were

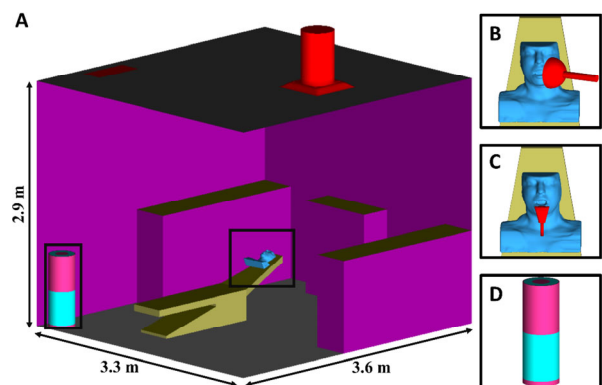


**Fig. 1** (A) Geometry of the dental clinic showing the locations of the extra-oral suction devices and HEPA filtration unit; (B) extra-oral suction device #1; (C) extra-oral suction device #2; (D) HEPA filtration unit.

performed for ventilation rates of 6.3, 9, 12, 15, and 18 ACH. Simulations were also performed to investigate the four speeds of the portable HEPA filtration unit, namely 4333 L/min (low speed), 6513 L/min (medium speed), 8835 L/min (high speed), and 11,497 L/min (turbo speed). The flow rates of the extra-oral suction devices #1 and #2 are unknown. Preliminary simulations were performed to identify the flow rate threshold above which these devices effectively scrubbed all particles emanating from the patient's mouth. The final simulations were performed with flow rates of 0, 50, 150, 200, 250, 400, 600, and 800 L/min for the two extra-oral suction devices. The computational mesh included all three devices, but each device was studied separately while keeping the flow rates of the other two devices equal to zero (Table 1).

## 2.2 Computational fluid dynamics—airflow simulations

The CFD simulations were performed in ANSYS Fluent 2020 R2. The geometry of the dental clinic was created in ANSYS ICEM-CFD. To transfer the geometry from ICEM-CFD to Fluent, a tetrahedral mesh was created, exported in “.msh” format, and imported into Fluent. A polyhedral mesh was created in Fluent Meshing with five prism layers. The mesh was graded near the patient's mouth, the inlet vent, and the extra-oral suction devices to accurately capture the airflow patterns (Fig. 2). The mesh size was selected via a mesh density study (see Section 3 Results). Steady-state airflow simulations were performed

with the  $k$ - $\omega$  turbulence model using an air density of  $1.2 \text{ kg/m}^3$  and air viscosity of  $1.8 \times 10^{-5} \text{ kg/(m}\cdot\text{s)}$ . A pressure-inlet boundary condition was used to impose atmospheric pressure at the inlet vent on the ceiling. A mass flow outlet boundary condition with a mass flow rate of  $0.0708 \text{ kg/s}$  (corresponding to the room ventilation of 6.3 ACH) was applied at the outlet vent on the ceiling. Mass flow inlet and mass flow outlet boundary conditions were applied at the inlet and outlet of the HEPA filtration unit, while a mass flow outlet boundary condition was applied at the outlet of the extra-oral suction devices in simulations representing these devices turned on. The coupled scheme was used for the pressure-velocity coupling and second-order discretization was used for all partial differential equations.

## 2.3 Computational fluid dynamics—particle transport simulations

Dental instrumentation generates a particle cloud with complex dynamics. Particles are released in varying directions as the dentist moves the instrumentation along the patient's teeth. Furthermore, continuous release of a large number of particles generates a particle cloud that transfers momentum to the surrounding air. Simulating all this complexity would require simulating different positions of the dental instrumentation, knowledge of the precise particle size distribution, and performing two-way particle transport simulations. In this work we adopt a simplified

**Table 1** Description of the flow rates investigated (each device studied separately)

Case	Description of case	Flow rates studied
1	Standard of care (no device operating, only room ventilation)	6.3, 9, 12, 15, and 18 ACH
2	Only extra-oral suction device #1 with 6.3 ACH room ventilation	0, 50, 150, 200, 250, 400, 600, and 800 L/min
3	Only extra-oral suction device #2 with 6.3 ACH room ventilation	0, 50, 150, 200, 250, 400, 600, and 800 L/min
4	Only HEPA filtration unit with 6.3 ACH room ventilation	4333, 6513, 8835, and 11,497 L/min

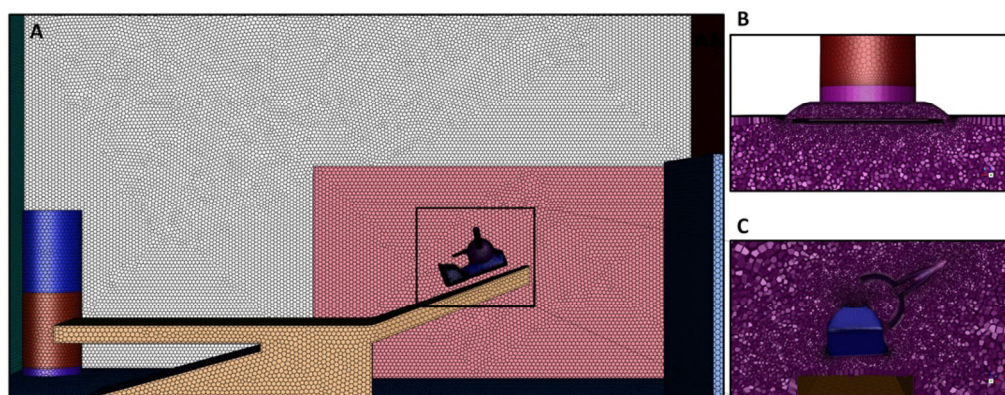


**Fig. 2** (A) Polyhedral mesh of the dental clinic with five prism layers; (B) mesh refined near the ventilation inlet on the ceiling; (C) mesh refined around the patient's mouth and extra-oral suction devices.

approach, which nonetheless allows us to investigate the efficacy of aerosol mitigation strategies. Particles were released with an initial velocity of 7 m/s perpendicular to a circular surface at the center of the patient’s mouth. The velocity of 7 m/s is a median of the particle velocity range of 2–12 m/s reported for dental instrumentation (dental drilling, ultrasonic scaler, and 3-in-1 air water syringe) (Eames et al., 2021; Haffner et al., 2021; Li et al., 2021; Sergis et al., 2021; Ohya et al., 2022). An inlet-velocity boundary condition with air velocity of 7 m/s was imposed at this circular release surface to approximate the momentum transfer from particles to the surrounding air. The diameter of the circular release surface (6.8 mm) was selected so that the volume flow rate emanating from the patient’s mouth was 15 L/min, which is similar to the exhalation rate of an adult at rest.

Spherical particles of diameters from 0.3 to 10 μm were investigated using 16 log-spaced particle size bins (Table 2). This particle size range represents small droplets that can remain suspended in air for an extended period of time as opposed to larger particles (diameter > 10 μm) that tend to deposit near the patient’s mouth due to gravitational settling. This range of particle sizes with 16 size bins was selected because it is commonly used in instrumentation to monitor aerosol concentrations (Allison et al., 2021, 2022; Sergis et al., 2021; Vernon et al., 2021; Ye et al., 2021; Fennelly et al., 2022). The particles had a density (ρ) of 1000 kg/m<sup>3</sup> so that the geometric diameter was equivalent to the aerodynamic diameter. The discrete phase model in

**Table 2** Particle frequency distribution used in this study to represent the aerosol generated by dental drilling based on the experimental data in Fig. 3 (Vernon et al., 2021)

<i>d</i> (μm)	<i>f<sub>d</sub></i>
0.3368	0.3178
0.4193	0.2170
0.5220	0.1482
0.6499	0.1012
0.8092	0.0691
1.0074	0.0472
1.2543	0.0322
1.5616	0.0220
1.9443	0.0150
2.4207	0.0103
3.0138	0.0070
3.7523	0.0048
4.6717	0.0033
5.8164	0.0022
7.2416	0.0015
9.0160	0.0010

ANSYS Fluent accounted for the acceleration of gravity and buoyancy effects. The particles were assumed to be inert (i.e., particle evaporation was not considered). Thus, our CFD simulations represent dental drilling, but do not represent procedures that generate water droplets where it is important to consider droplet evaporation (Komperda et al., 2021). A trap boundary condition was applied on all walls and an escape boundary condition was applied at all outlets, including the device outlets.

Dental instrumentation generates polydisperse aerosols. Here, we adopt the particle size distribution reported by Vernon et al. (2021), observed during drilling with an air turbine without the use of aerosol mitigation devices (Fig. 3).

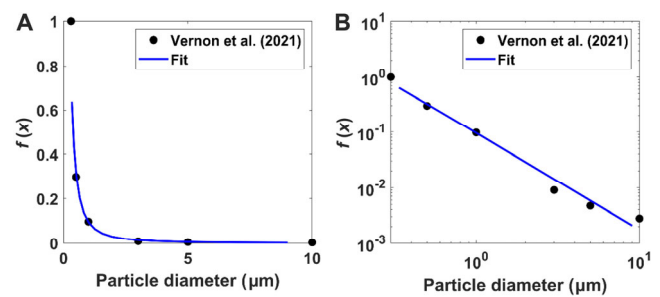


**Fig. 3** Particle count distribution generated by dental drilling with an air turbine in the absence of aerosol mitigation strategies: (A) linear scale; (B) log–log scale (Vernon et al., 2021).

The particle count distribution reported by Vernon et al. (2021) is well-represented by the power law fit  $f(x) = ax^b$ , where the constants  $a = 0.096$  and  $b = -1.74$  were estimated with a linear regression of the linearization  $\log(f(x)) = \log(a) + b\log(x)$  (Pearson  $r = -0.991$ ) (Fig. 3). This particle count distribution was used to obtain the frequency distribution  $f_d$  of the 16 particle sizes simulated (Table 2) with the definition:

$$\sum_{d=1}^{16} f_d = 1 \tag{1}$$

where  $f_d$  is the fraction of the aerosol cloud that is composed of particles with diameter  $d$ .

### 2.4 Estimation of PM<sub>10</sub>

The aerosol concentration in the dental clinic was quantified as the particulate matter under 10 μm in aerodynamic diameter (PM<sub>10</sub>) in μg/m<sup>3</sup>, namely

$$PM_{10}(t) = \sum_{d=1}^{16} \frac{M_d(t)}{V} = \frac{1}{V} \sum_{d=1}^{16} M_d(t) \tag{2}$$

where  $V = 33.9 \text{ m}^3$  is the volume of air in the dental clinic and  $M_d(t)$  is the total mass of particles of diameter  $d$  that

remain airborne at time  $t$ . The sum in Eq. (2) is performed over the 16 particle diameters simulated. The total mass of particles of diameter  $d$  that remains airborne at time  $t$  is

$$M_d(t) = m_d N_d(t) \tag{3}$$

where  $N_d(t)$  is the number of particles of diameter  $d$  that remain airborne at time  $t$ , and  $m_d = \rho \frac{4}{3} \pi \left(\frac{d}{2}\right)^3 = \rho \frac{\pi}{6} d^3$  is the mass of one spherical particle of diameter  $d$ , where  $\rho$  is the particle density.

Rather than simulating the exact number of particles released during a dental procedure, we simulated a total of  $(N_T)_{CFD}$  particles. The particles were released from a grid of uniformly spaced release points inside the circular release surface. One particle of each diameter was released from each release point so that the total number of particles simulated was

$$(N_T)_{CFD} = 16N_{rp} \tag{4}$$

where 16 is the number of particle diameters simulated and  $N_{rp}$  is the number of release points. The number of release points was selected by performing a parameter sensitivity analysis (see Section 3 Results).

We simulated a scenario of 15 min of dental drilling followed by 30 min of a resting period. The steady-state CFD simulations quantified the trajectories of a single packet of  $(N_T)_{CFD}$  particles and provided the time  $t_i$  when each particle deposited on a surface or exited the fluid domain via the outlet vent, the HEPA filtration unit, or the extra-oral suction devices. A MATLAB code was developed to read the time  $t_i$  from text files (.dpm files) generated by ANSYS Fluent and compute the time evolution of  $PM_{10}(t)$ . The MATLAB code assumed that a new packet of  $(N_T)_{CFD}$  particles was released from the patient’s mouth every second during the dental drilling procedure. The number of particles of diameter  $d$  airborne at time  $t + \Delta t$  was computed from Eq. (5):

$$N_d(t + \Delta t) = N_d(t) + N_{added}^d - N_{removed}^d \tag{5}$$

where  $\Delta t = 1$  s is the time step,  $N_{added}^d$  is the number of particles of diameter  $d$  released per second, and  $N_{removed}^d$  is the number of particles of diameter  $d$  that deposited or exited the fluid domain during the time interval from  $t$  to  $t + \Delta t$ . The number of particles of diameter  $d$  released per second was  $N_{added}^d = N_{rp}$  for the duration of the drilling procedure ( $t = 0-15$  min) and  $N_{added}^d = 0$  during the resting period ( $t = 15-45$  min). The number of particles of diameter  $d$  removed in each time interval ( $N_{removed}^d$ ) was computed from the CFD results considering that a new packet of  $(N_T)_{CFD}$  particles was released every second during the

15 min of dental drilling and using the duration of each particle trajectory.

Since we did not simulate the exact number of particles released during a dental procedure, it was necessary to convert the number of particles simulated to the number observed in the dental procedure via a scaling factor. First, we notice that the concentration of particles in air is proportional to the mass of particles released per second, namely

$$\frac{(PM_{10})_{EXP}}{(PM_{10})_{CFD}} = \frac{(M_T)_{EXP}}{(M_T)_{CFD}} = k_1 \tag{6}$$

where  $(PM_{10})_{CFD}$  and  $(PM_{10})_{EXP}$  are respectively the particle concentrations in air predicted by the CFD simulation and observed during a dental procedure (i.e., experimental conditions),  $(M_T)_{CFD}$  and  $(M_T)_{EXP}$  are respectively the total masses of particles released per second in the CFD simulation and during a dental procedure, and  $k_1$  is a constant. Using the particle frequency distribution generated by dental drilling (Table 2), the total mass of particles released per second in a dental procedure is

$$\begin{aligned} (M_T)_{EXP} &= \sum_{d=1}^{16} m_d (N_d^0)_{EXP} = \sum_{d=1}^{16} m_d f_d (N_T)_{EXP} \\ &= (N_T)_{EXP} \sum_{d=1}^{16} m_d f_d \end{aligned} \tag{7}$$

where  $(N_d^0)_{EXP} = f_d (N_T)_{EXP}$  is the number of particles of diameter  $d$  released per second in the experiments and  $(N_T)_{EXP}$  is the total number of particles released per second in the experiments. Meanwhile, the total mass of particles released per second in the CFD simulation is

$$\begin{aligned} (M_T)_{CFD} &= \sum_{d=1}^{16} m_d (N_d^0)_{CFD} = \sum_{d=1}^{16} m_d \frac{(N_T)_{CFD}}{16} \\ &= \frac{(N_T)_{CFD}}{16} \sum_{d=1}^{16} m_d \end{aligned} \tag{8}$$

where  $(N_d^0)_{CFD} = \frac{1}{16} (N_T)_{CFD}$  is the number of particles of diameter  $d$  released per second in the CFD simulations. Substituting Eqs. (7) and (8) into Eq. (6), we find

$$\frac{(PM_{10})_{EXP}}{(PM_{10})_{CFD}} = \frac{(N_T)_{EXP}}{(N_T)_{CFD}} k_2 = k_1 \tag{9}$$

where

$$k_2 = \frac{\sum_{d=1}^{16} m_d f_d}{\frac{1}{16} \sum_{d=1}^{16} m_d} \tag{10}$$

is a constant determined by the particle size distribution.

Next, we notice that the number of particles that remain airborne at time  $t$  is proportional to the number of particles released, so that

$$\frac{(N_d)_{\text{EXP}}(t)}{(N_d)_{\text{CFD}}(t)} = \frac{(N_d^0)_{\text{EXP}}}{(N_d^0)_{\text{CFD}}} \tag{11}$$

where  $(N_d)_{\text{CFD}}(t)$  and  $(N_d)_{\text{EXP}}(t)$  are the numbers of particles of diameter  $d$  that remain airborne at time  $t$  in the CFD simulations and experiments, respectively. Using the particle frequency distribution generated by dental drilling (Table 2), we have

$$(N_d^0)_{\text{EXP}} = f_d (N_T)_{\text{EXP}} \tag{12}$$

Meanwhile, the number of particles of diameter  $d$  released per second in the CFD simulations is equal to the number of release points:

$$(N_d^0)_{\text{CFD}} = N_{\text{rp}} = \frac{1}{16} (N_T)_{\text{CFD}} \tag{13}$$

where we used Eq. (4). Substituting Eqs. (12) and (13) into Eq. (11), we have

$$(N_d)_{\text{EXP}}(t) = 16(k_1/k_2) f_d (N_d)_{\text{CFD}}(t) \tag{14}$$

where we used  $\frac{(N_T)_{\text{EXP}}}{(N_T)_{\text{CFD}}} = \frac{k_1}{k_2}$  from Eq. (9). Finally, using Eqs. (2), (3), and (14), we find that the particle concentration in air in the dental clinic is given by

$$(PM_{10})_{\text{EXP}}(t) = \frac{16 k_1}{V k_2} \sum_{d=1}^{16} f_d m_d (N_d)_{\text{CFD}}(t) \tag{15}$$

where the rescaling factor  $k_1$ , which accounts for the fact that the CFD simulations were performed with less particles than the actual number of particles released during the dental drilling procedure, is given by Eq. (9):

$$k_1 = \frac{(PM_{10})_{\text{EXP}}}{(PM_{10})_{\text{CFD}}} \tag{16}$$

In this work, we assume that 15 min of a dental drilling procedure generates an air concentration of  $(PM_{10})_{\text{EXP}} = 30 \mu\text{g}/\text{m}^3$  based on the experimental measurements by Sotiriou et al. (2008) in the absence of aerosol mitigation devices (Sotiriou et al., 2008). Readers should note that our CFD simulations assumed that the air entering the dental clinic through the inlet vent on the ceiling had zero particles, when in reality the air in ventilation systems always has a background particle concentration. Therefore, our CFD simulations represent the excess  $PM_{10}$  generated by dental drilling—i.e., the additional particle concentration above the background level. The efficiency of aerosol mitigation strategies was quantified by the scrubbing time, which was defined as the amount of time required to remove 95% of the aerosol released during the dental procedure.

### 3 Results

#### 3.1 Verification of the CFD model

Polyhedral meshes were created with maximum cell sizes of 30, 22, and 20 mm, which provided three mesh sizes, namely 3.3 million cells (coarse mesh), 6.2 million cells (medium mesh), and 8.7 million cells (fine mesh). The mesh resolution of the circular release surface (1 mm), 3D reconstruction of the patient’s head (10 mm), inlet vent (10 mm), extra-oral suction device #1 (4 mm), extra-oral suction device #2 (1 mm), and HEPA filtration unit (20 mm) were kept fixed to provide a higher mesh resolution at these locations.

Airflow simulations were performed in the baseline case (i.e., zero flow through the devices). The air velocity magnitude was investigated along two lines, namely a vertical line from the patient’s mouth to the ceiling and a horizontal line crossing the patient’s mouth laterally. Reasonable agreement was observed for the air velocity magnitude predicted by the three meshes (Fig. 4).

A colormap of air velocity magnitude in the baseline case showed that air velocity was almost 0 m/s in most of

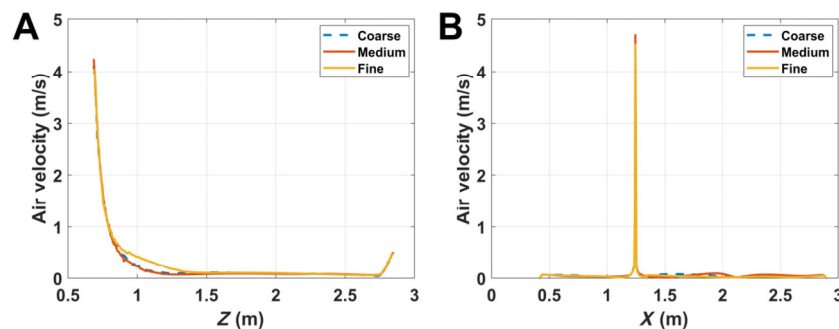


**Fig. 4** Grid independence study showing good agreement for three mesh resolutions (coarse, medium, fine) for air velocity calculated along (A) a vertical line from the patient’s mouth to the ceiling and (B) a horizontal line crossing the patient’s mouth laterally.

the space in the dental office, except near the ceiling due to the inlet vent and near the patient’s mouth due to the plume of air and particles emanating from the patient’s mouth (Figs. 5(A) and 6(A)). Likewise, the plot of air velocity magnitude along the horizontal line showed that the air was quiescent in most of the dental clinic, except near the patient’s mouth (Fig. 4(B)). This flow pattern was captured by all three meshes (Fig. 4). However, some differences in air velocity magnitude were observed among the meshes, especially along the vertical line (Fig. 4(A)). This suggested that the airflow field was not entirely mesh-independent.

Discrete phase model (DPM) simulations were also performed to quantify the impact of mesh resolution on the predicted  $PM_{10}$ . These simulations were performed in the case with extra-oral suction device #1 using four different flow rates (0, 250, 500, and 1000 L/min). Reasonable

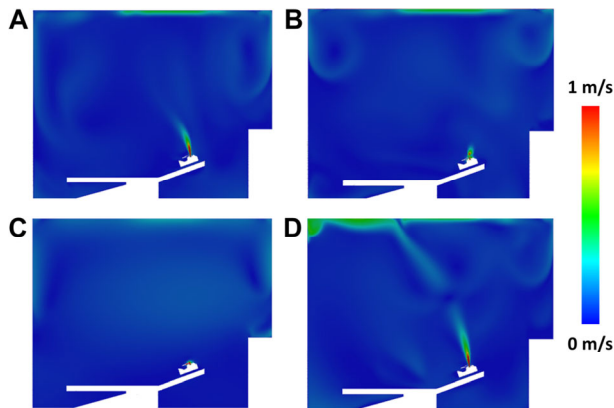


**Fig. 5** Colormap of velocity magnitude for a plane crossing through the patient’s mouth showing reduction in airflow exiting the patient’s mouth when the extra-oral devices are used. (A) Baseline condition; (B) extra-oral suction device #1 operating at 200 L/min; (C) extra-oral suction device #2 operating at 200 L/min; (D) HEPA filtration unit operating at 4333 L/min.

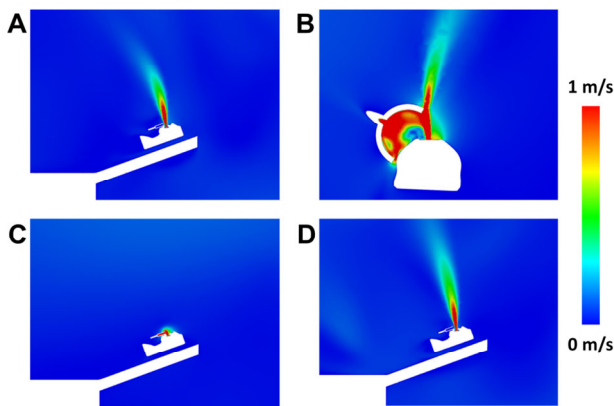


**Fig. 6** Colormap of velocity magnitude illustrating the airflow field near the patient’s mouth. (A) Baseline condition; (B) extra-oral suction device #1 operating at 200 L/min; (C) extra-oral suction device #2 operating at 200 L/min; (D) HEPA filtration unit operating at 4333 L/min.

agreement was observed for the three mesh resolutions with the peak  $PM_{10}$  observed at the end of the dental drilling procedure (time = 15 min) decreasing from the baseline of 30 to 0  $\mu\text{g}/\text{m}^3$  when the flow rate of extra-oral suction device #1 exceeded 500 L/min in all three meshes (Fig. 7). However, some variability was observed between the coarse, medium, and fine meshes when the flow rate of extra-oral suction device #1 was 250 L/min (Fig. 7). Based on these results, we concluded that the fine mesh provided an airflow field and particle tracking results that were nearly, but not entirely, mesh-independent. The fine mesh was the highest resolution that could be created in our local workstation due to a memory limitation (32 GB of RAM memory). Therefore, all subsequent CFD simulations were performed in the fine mesh.

A parameter sensitivity analysis was also performed to investigate how changes in the number of release points used in the DPM simulations affected the predicted  $PM_{10}$ . Simulations were performed with 500, 1000, 2000, 4000, or 8000 release points in the baseline case. Changes in the number of release points had a negligible impact on the temporal evolution of  $PM_{10}$  (Fig. 8). Thus, a value of  $N_{rp} = 2000$  release points was used in all subsequent simulations.

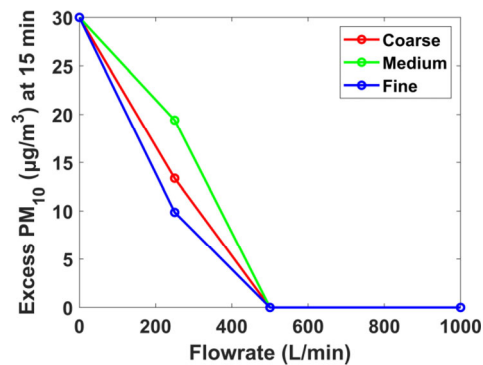


**Fig. 7** Grid independence study showing that  $PM_{10}$  reduced to zero when the flow rate of extra-oral suction device #1 exceeded 500 L/min. This result was independent of the mesh density, but  $PM_{10}$  was sensitive to mesh density for a flow rate of 250 L/min.

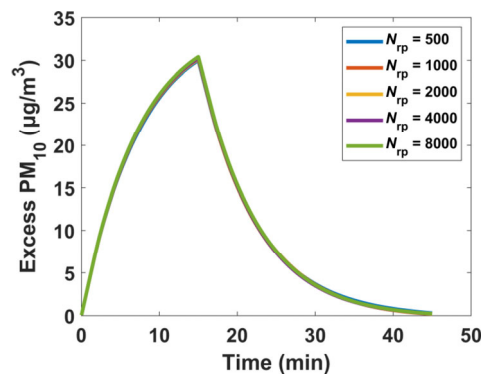


**Fig. 8** Parameter-sensitivity study showing that  $PM_{10}$  was nearly independent of the number of particle release points ( $N_{rp}$ ).



### 3.2 Airflow pattern

It is important to understand the airflow pattern inside the dental clinic since this is a crucial factor determining the particle trajectories and evolution of  $PM_{10}$ . Figures 5 and 6 compare the colormap of air velocity magnitude in the baseline case and in the cases with the extra-oral suction devices and HEPA filtration unit operating. In all cases, airflow coming from the inlet vent on the ceiling flows along the ceiling until it reaches the walls, where low-velocity flow vortices are formed. The tendency of an airflow jet emerging from an orifice to flow along an adjacent surface is known as the “Coanda effect”, and is explained by the ambient pressure pushing the lower pressure incoming jet against the ceiling. Consequently, air velocity in the center of the room has a low magnitude except for the air jet emanating from the patient’s mouth (Figs. 5(A) and 6(A)). Simulations with the extra-oral suction devices #1 and #2 operating at a flow rate of 200 L/min show a significant reduction in the jet emanating from the patient’s mouth because the air is sucked by the devices (Figs. 5(B) and 5(C)). In contrast, the simulation with the HEPA filtration unit operating at a flow rate of 4333 L/min shows an air jet emanating from the patient’s mouth similar to the baseline condition, but there is an increase in the air velocity near the ceiling as the HEPA filtration unit blows filtered air from its top surface toward the ceiling (Fig. 5(D)). Overall, the elliptical extra-oral suction device #2 had the best performance

(Figs. 5(C) and 6(C)) in terms of reducing the air jet emanating from the patient’s mouth.

### 3.3 Aerosol concentration in the dental clinic

In the baseline case with a ventilation of 6.3 ACH,  $PM_{10}$  increased steadily and reached  $30 \mu\text{g}/\text{m}^3$  after 15 min of dental drilling, and then declined steadily reaching  $0.2 \mu\text{g}/\text{m}^3$  at the end of the 30 min resting period (Fig. 9(A)). Increasing the room ventilation from 6.3 to 18 ACH reduced the peak  $PM_{10}$  from 30 to  $10.1 \mu\text{g}/\text{m}^3$  (Figs. 9(A) and 10(A)). This increase in room ventilation reduced the scrubbing time from 20.5 to 4.5 min (Fig. 11).

In the case with the extra-oral suction device #1, increasing the device flow rate had almost no impact on  $PM_{10}$  for device flow rates below 200 L/min (Figs. 9(B) and 10(B)). When the device flow rate exceeded 200 L/min, a sharp reduction in aerosol concentration was observed with  $PM_{10}$  decreasing to  $0 \mu\text{g}/\text{m}^3$  for flow rates above 400 L/min. A similar behavior was observed in the case with extra-oral suction device #2, except that the sudden reduction in  $PM_{10}$  was observed at a smaller device flow rate and  $PM_{10}$  decreased to  $0 \mu\text{g}/\text{m}^3$  for device flow rates above 150 L/min (Figs. 9(C) and 10(C)).

In the case with the HEPA filtration unit, operating the device at its lowest speed (4333 L/min) reduced the peak  $PM_{10}$  from the value of  $30 \mu\text{g}/\text{m}^3$  observed in the baseline case to  $18.1 \mu\text{g}/\text{m}^3$  (Figs. 9(D) and 10(D)). Increasing the

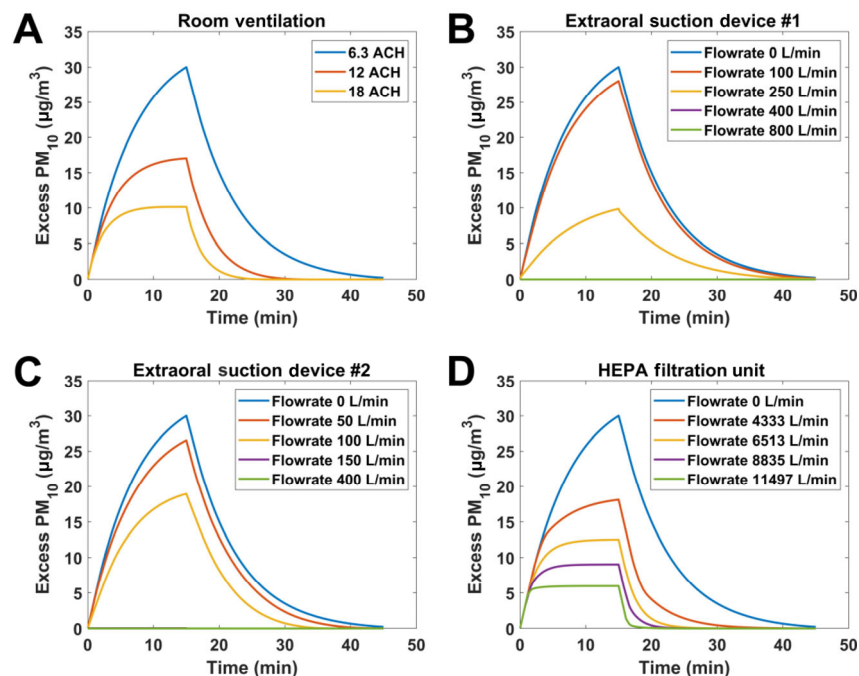


**Fig. 9** Evolution of  $PM_{10}$  during 15 min of dental drilling followed by a 30 min resting period. (A) Effect of increasing room ventilation, which is measured in ACH; (B) effect of increasing the flow rate of extra-oral suction device #1; (C) effect of increasing the flow rate of extra-oral suction device #2; (D) effect of increasing the flow rate of the HEPA filtration unit.

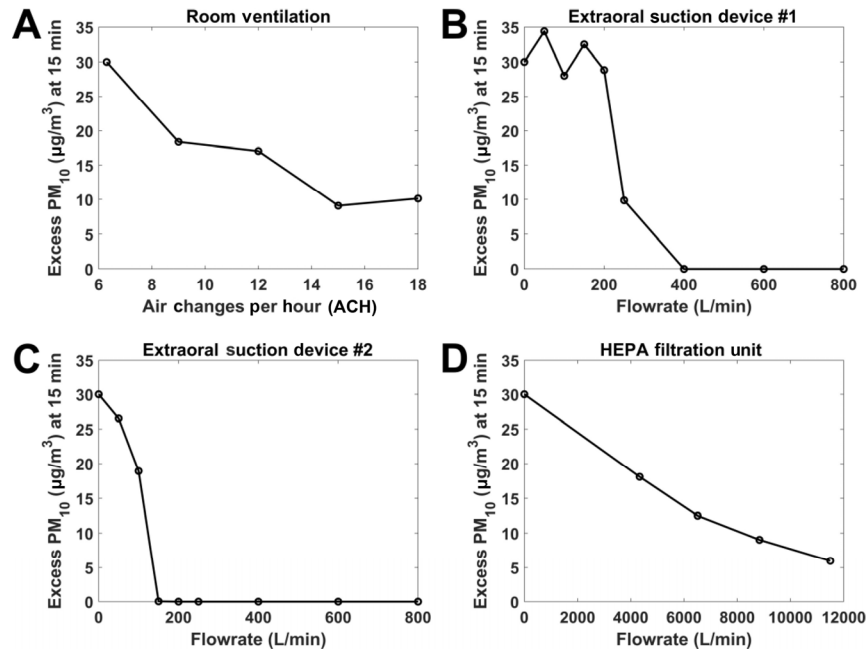


**Fig. 10** PM<sub>10</sub> after 15 min of dental drilling as a function of (A) room ventilation, (B) flow rate of extra-oral suction device #1, (C) flow rate of extra-oral suction device #2, and (D) flow rate of the HEPA filtration unit.

flow rate of the HEPA filtration unit to its maximum speed (11,497 L/min) further reduced the peak PM<sub>10</sub> to 6.0 µg/m<sup>3</sup>. The scrubbing time was predicted to decrease from 9.8 min at the lowest speed to 1.1 min at the highest speed of the HEPA filtration unit (Fig. 11). The highest speed of the HEPA filtration unit was equivalent to 20.3 ACH. When combined with the room ventilation of 6.3 ACH, the rate of air replacement of the dental clinic was 26.6 ACH. Consequently, the scrubbing time of 1.1 min predicted for the highest speed of the HEPA filtration unit was lower than the scrubbing time of 4.5 min predicted for the highest room ventilation of 18 ACH in the absence of aerosol mitigation devices (Fig. 11).

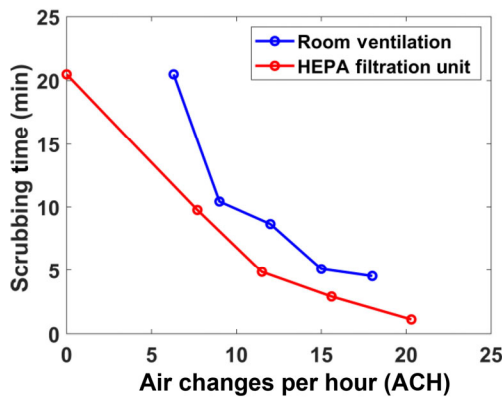


**Fig. 11** Scrubbing time (i.e., amount of time required to remove 95% of the aerosol released during the dental procedure) as a function of the room ventilation and the flow rate of the HEPA filtration unit expressed in ACH.

To further interpret these results, we quantified the volume-averaged air velocity in a 25-mm-diameter spherical region in front of the patient’s mouth. This volume-averaged air velocity ( $\bar{v}$ ) was approximately linearly related to the flow rate of the extra-oral suction devices (Figs. 12(B) and 12(C)). Increasing the flow rate of the extra-oral suction device #1 increased the volume-averaged air velocity from 0.33 to 1.7 m/s when the device flow rate increased from 0 to 800 L/min (Fig. 12(B)). Similarly, increasing the flow rate of the extra-oral suction device #2 increased the volume-averaged air velocity from 0.33 to 4.1 m/s when the device flow rate increased from 0 to 800 L/min (Fig. 12(C)). The greater air velocity generated by the extra-oral suction device #2 is explained by the smaller cross-sectional area of its suction cup.

In both cases, PM<sub>10</sub> reduced to 0 µg/m<sup>3</sup> when the volume-averaged air velocity in front of the patient’s mouth exceeded approximately  $\bar{v} = 0.9$  m/s (Figs. 13(B) and 13(C)). Smaller changes in air velocity were observed in front of the patient’s mouth in simulations varying the room ventilation and the flow rate of the HEPA filtration unit. Specifically, increasing room ventilation from 6.3 to 18 ACH increased  $\bar{v}$  only from 0.33 to 0.42 m/s (Fig. 12(A)), and increasing the flow rate of the HEPA filtration unit from 0 to 11,497 L/min increased  $\bar{v}$  only from 0.33 to 0.36 m/s (Fig. 12(D)). This illustrates the different mechanisms of aerosol mitigation strategy, namely the extra-oral suction devices scrub the aerosol plume at its source, while room ventilation replaces the aerosol-laden

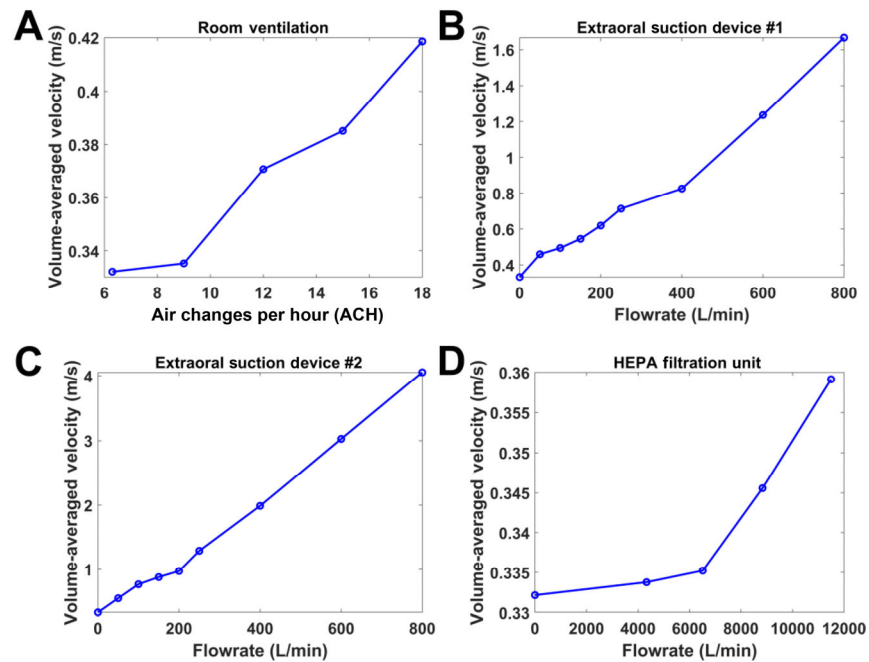


**Fig. 12** Air velocity averaged over a 25-mm-diameter sphere in front of the patient's mouth as a function of (A) room ventilation, (B) flow rate of extra-oral suction device #1, (C) flow rate of extra-oral suction device #2, and (D) flow rate of the HEPA filtration unit.

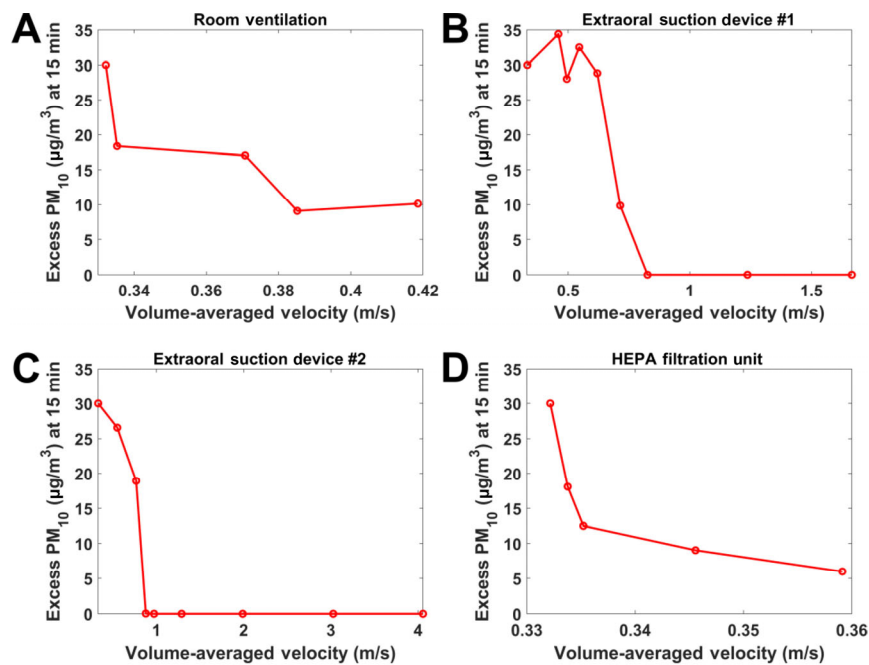


**Fig. 13** PM<sub>10</sub> after 15 min of dental drilling as a function of the air velocity in front of the patient's mouth for the cases of increasing (A) room ventilation and flow rate of (B) extra-oral suction device #1, (C) extra-oral suction device #2, and (D) the HEPA filtration unit.

air in the dental clinic with clean air, and the HEPA filtration unit filters the aerosol-laden air and returns the filtered air to the room.

#### 4 Discussion

To our knowledge, this is the first study to apply CFD to

quantify the relative efficacy of extra-oral suction devices, HEPA filtration units, and room ventilation to reduce dental aerosols. A major innovation of this study is the development of a numerical method to compute PM<sub>10</sub>. Previous studies have applied CFD to investigate particle dispersion in dental clinics (Komperda et al., 2021) and how to optimize ventilation in hospital rooms (Méndez et al.,

2008; Bhattacharyya et al., 2020), but these studies only reported the aerosol removal efficiency for specific particle sizes or the air replacement rate.  $PM_{10}$  is likely a better metric to assess the risk of disease transmission than a single particle size because  $PM_{10}$  is the total concentration of airborne particles with aerodynamic diameters below 10  $\mu\text{m}$ . A recent review of the assumptions in numerical studies of airborne virus transmission stated that it is essential to incorporate the particle size distribution for realistic predictions of disease transmission risk (Pourfatah et al., 2021).

Experimental studies have reported that extra-oral suction devices are effective strategies to reduce aerosol dispersion in dental clinics, with some studies reporting greater than 90% reduction in aerosol concentration (Allison et al., 2022; Fennelly et al., 2022) while other studies reported a more modest reduction of 38%–86% (Ou et al., 2021; Remington et al., 2022). These experimental studies cannot be directly compared to our CFD results because they did not report  $PM_{10}$ , but rather used different metrics of aerosol concentration, such as particle counts. Nevertheless, these experimental observations contrast to our prediction of 100% aerosol removal efficiency for device flow rates above 400 L/min (Fig. 10). Importantly, the distance from the suction cup to the mouth was 0–2 cm in our study, but ranged from 10 to 20 cm in these experimental studies. The crucial importance of the suction cup position was demonstrated by Ou et al. (2021), who reported that when the suction cup was moved 4 cm further away (from 14 to 18 cm from the mouth), its capture efficiency dropped from 74% to 38% at a device flow rate of 1670 L/min, and from 96% to 56% at a device flow rate of 3653 L/min. Additional studies are needed to characterize how the suction cup position affects the aerosol removal efficiency of extra-oral suction devices.

Several limitations of this study must be acknowledged. First, our numerical methods did not account for thermal and humidity effects, such as evaporating droplets and changes in air density, that may affect the evolution of  $PM_{10}$ . Second, our CFD simulations were not entirely mesh-independent. Nevertheless, our mesh density test suggests that the main conclusions of this study are valid. Third, this study did not investigate systematically how the shape of the suction cup of extra-oral suction devices affects the aerosol removal efficiency. The shapes of the extra-oral suction devices #1 and #2 were different (circular vs. elliptical), but their positions were also different (lateral vs. inferior to the mouth). The fact that the device flow rate at which  $PM_{10}$  decreased to 0  $\mu\text{g}/\text{m}^3$  had a similar magnitude in the two extra-oral suction devices (Fig. 10) suggests that the device flow rate is the most important parameter determining the efficacy of extra-oral suction devices. This

hypothesis is supported by a previous CFD study which found that the shape of the suction cup has a relatively small impact on the aerosol removal efficiency (Liu et al., 2022). Additional studies are needed to investigate the importance of the shape of the suction cup.

Fourth, our study did not quantify spatial variations in  $PM_{10}$  that can lead to higher aerosol concentrations near the patient and dental healthcare workers. We estimated  $PM_{10}$  based on the duration of particle trajectories without knowledge of the actual path that each particle traveled. In other words, our computational method assumed an equal concentration throughout the room (i.e., a well-mixed gas), when in reality the aerosol concentration is expected to be higher near the patient. Holliday et al. (2021) performed a crown preparation on a mannequin with fluorescein dye introduced either into the mannequin's mouth or the irrigation system. Filter papers placed up to 6 m from the mannequin demonstrated contamination at large distances from the mannequin, but with higher contamination in the mannequin's vicinity. Grenier (1995) used agar plates to investigate bacterial contamination in a multi-chair clinic at a dental school. Bacterial contamination was detected 11 m away from where dental activity occurred, but at a lower level than in the area where patients were treated. While these studies confirm the expectation that aerosol concentration is higher near the patient, our review of the literature suggests that most experimental studies sampled the air at a single site and did not investigate spatial variations in aerosol concentration. Future studies should investigate the degree of spatial variation in  $PM_{10}$ , which can influence the transmission risk of airborne pathogens.

Another limitation of this work is that only a single location of the HEPA filtration unit was investigated. A previous CFD study by Chen et al. (2010) demonstrated that the aerosol removal efficiency of an air cleaner was determined by the combination of its location and direction of airflow. In our study, the HEPA filtration unit was positioned at the corner of the room based on the dentists' judgment that this location was the least intrusive for clinical care. The HEPA filtration unit we investigated pulls air from its sides and returns the filtered air through its top. Additional studies are needed to investigate how the design and location of HEPA filtration units impact their aerosol removal efficiency.

Finally, the efficacy of increasing room ventilation to reduce aerosols is dependent on the design of the dental clinic, including the positions of the dental chair, inlet vent, and outlet vent. Memarzadeh and Xu (2012) reported that the path from the contamination source to the outlet vent was more important than the ventilation rate in determining contaminant removal (Memarzadeh and Xu, 2012).

## 5 Conclusions

In summary, to our knowledge, this is the first CFD study to quantify the evolution of PM<sub>10</sub> in a dental clinic after a dental procedure. We investigated the efficacy of three strategies to reduce aerosol dispersion in dental clinics, namely increasing room ventilation, using a portable HEPA filtration unit, or using extra-oral suction devices. In the baseline simulation, PM<sub>10</sub> reached 30 µg/m<sup>3</sup> after 15 min of dental drilling, and it took 20.5 min for PM<sub>10</sub> to fall below 1.5 µg/m<sup>3</sup> (i.e., to remove 95% of the released aerosols) in a dental clinic with ventilation of 6.3 ACH. The scrubbing time reduced to under 5 min when the air exchange rate exceeded 15 ACH by either increasing the room ventilation or by increasing the flow rate of the HEPA filtration unit. The CFD simulations also demonstrated that extra-oral suction devices can be used to remove 100% of the particles released by using a suction cup in close proximity to the patient's mouth. This 100% aerosol removal efficiency is achieved when the flow rate of the extra-oral suction device exceeds 400 L/min, which corresponds to an air velocity of about 1 m/s in front of the patient's mouth. Additional research is needed to quantify how aerosol dispersion in dental clinics is affected by factors not investigated in this study, such as the location of the HEPA filtration unit and the distance from the extra-oral suction device's suction cup to the patient's mouth.

## Acknowledgements

This work was supported by the Advancing a Healthier Wisconsin Endowment (Grant No. AHW REP 5520597). We are grateful to Dr. Jonathan Komperda and Dr. Farzad Mashayek (Department of Mechanical and Industrial Engineering, University of Illinois at Chicago) for kindly sharing with us the geometry of the inlet vent. The authors are also grateful to Dr. Amin Zarandi for contributing to the preliminary CFD simulations for this project.

## Declaration of competing interest

The authors have no competing interests to declare that are relevant to the content of this article.

## References

- Allison, J. R., Dowson, C., Pickering, K., Červinskytė, G., Durham, J., Jakubovics, N. S., Holliday, R. 2022. Local exhaust ventilation to control dental aerosols and droplets. *Journal of Dental Research*, 101: 384–391
- Allison, J. R., Edwards, D. C., Bowes, C., Pickering, K., Dowson, C., Stone, S. J., Lumb, J., Durham, J., Jakubovics, N., Holliday, R. 2021. The effect of high-speed dental handpiece coolant delivery and design on aerosol and droplet production. *Journal of Dentistry*, 112: 103746.
- Bhattacharyya, S., Dey, K., Paul, A. R., Biswas, R. 2020. A novel CFD analysis to minimize the spread of COVID-19 virus in hospital isolation room. *Chaos, Solitons & Fractals*, 139: 110294.
- Chen, C., Zhao, B., Cui, W., Dong, L., An, N., Ouyang, X. 2010. The effectiveness of an air cleaner in controlling droplet/aerosol particle dispersion emitted from a patient's mouth in the indoor environment of dental clinics. *Journal of the Royal Society Interface*, 7: 1105–1118.
- Chuang, C. Y., Cheng, H. C., Yang, S., Fang, W., Hung, P. C., Chuang, S. Y. 2014. Investigation of the spreading characteristics of bacterial aerosol contamination during dental scaling treatment. *Journal of Dental Sciences*, 9: 294–296.
- Dudding, T., Sheikh, S., Gregson, F., Haworth, J., Haworth, S., Main, B. G., Shrimpton, A. J., Hamilton, F. W., Group, A., Ireland, A. J., et al. 2022. A clinical observational analysis of aerosol emissions from dental procedures. *PLoS One*, 17: e0265076.
- Eames, I., D'Aiuto, F., Shahreza, S., Javanmardi, Y., Balachandran, R., Hyde, M., Ng, Y. L., Gulabivala, K., Watson, S., Davies, H., et al. 2021. Removal and dispersal of biofluid films by powered medical devices: Modeling infectious agent spreading in dentistry. *iScience*, 24: 103344.
- Fennelly, M., Gallagher, C., Harding, M., Hellebust, S., Wenger, J., O'Sullivan, N., O'Connor, D., Prentice, M. 2022. Real-time monitoring of aerosol generating dental procedures. *Journal of Dentistry*, 120: 104092.
- Grenier, D. 1995. Quantitative analysis of bacterial aerosols in two different dental clinic environments. *Applied and Environmental Microbiology*, 61: 3165–3168.
- Haffner, E. A., Bagheri, M., Higham, J. E., Cooper, L., Rowan, S., Stanford, C., Mashayek, F., Mirbod, P. 2021. An experimental approach to analyze aerosol and splatter formations due to a dental procedure. *Experiments in Fluids*, 62: 202.
- Harrel, S. K., Molinari, J. 2004. Aerosols and splatter in dentistry: A brief review of the literature and infection control implications. *Journal of the American Dental Association*, 135: 429–437.
- Holliday, R., Allison, J. R., Currie, C. C., Edwards, D. C., Bowes, C., Pickering, K., Reay, S., Durham, J., Lumb, J., Rostami, N., et al. 2021. Evaluating contaminated dental aerosol and splatter in an open plan clinic environment: Implications for the COVID-19 pandemic. *Journal of Dentistry*, 105: 103565.
- Jungo, S., Moreau, N., Mazevet, M. E., Ejeil, A. L., Biosse Duplan, M., Salmon, B., Smail-Faugeron, V. 2021. Prevalence and risk indicators of first-wave COVID-19 among oral health-care workers: A French epidemiological survey. *PLoS One*, 16: e0246586.
- Klompas, M., Baker, M. A., Rhee, C. 2020. Airborne transmission of SARS-CoV-2: Theoretical considerations and available evidence. *JAMA*, 324: 441–442.
- Komperda, J., Peyvan, A., Li, D., Kashir, B., Yarin, A. L., Megaridis, C. M., Mirbod, P., Paprotny, I., Cooper, L. F., Rowan, S., et al. 2021. Computer simulation of the SARS-CoV-2 contamination risk in a large dental clinic. *Physics of Fluids*, 33: 033328.

- Kumar, P. S., Subramanian, K. 2020. Demystifying the mist: Sources of microbial bioload in dental aerosols. *Journal of Periodontology*, 91: 1113–1122.
- Leggat, P. A., Kedjarune, U. 2001. Bacterial aerosols in the dental clinic: A review. *International Dental Journal*, 51: 39–44.
- Li, X., Mak, C. M., Ma, K. W., Wong, H. M. 2021. Evaluating flow-field and expelled droplets in the mockup dental clinic during the COVID-19 pandemic. *Physics of Fluids*, 33: 047111.
- Liu, P. 2022. Computational Fluid Dynamics Optimization of an Extraoral Vacuum Aerosol Cup for Airborne Disease Control in Dental Offices. *Aerosol Science and Engineering*, 6: 21–29. Available at <https://doi.org/10.1007/s41810-021-00121-6>.
- Meethil, A. P., Saraswat, S., Chaudhary, P. P., Dabdoub, S. M., Kumar, P. S. 2021. Sources of SARS-CoV-2 and other microorganisms in dental aerosols. *Journal of Dental Research*, 100: 817–823.
- Memarzadeh, F., Xu, W. 2012. Role of air changes per hour (ACH) in possible transmission of airborne infections. *Building Simulation*, 5: 15–28.
- Méndez, C., San José, J. F., Villafruela, J. M., Castro, F. 2008. Optimization of a hospital room by means of CFD for more efficient ventilation. *Energy and Building*, 40: 849–854.
- Natapov, L., Schwartz, D., Domb Herman, H., Dekel Markovich, D., Yellon, D., Jarallah, M., Liphshiz, I., Carmeli, Y., Karakis, I. 2021. Risk of SARS-CoV-2 transmission following exposure during dental treatment—A national cohort study. *Journal of Dentistry*, 113: 103791.
- Ohya, T., Nakagawa, K., Arai, Y., Kato, H. 2022. Visualization of droplets produced by dental air turbines that require infection control measured during coronavirus 2019 outbreaks. *Journal of Hospital Infection*, 119: 196–198.
- Ou, Q., Placucci, R. G., Danielson, J., Anderson, G., Olin, P., Jardine, P., Madden, J., Yuan, Q., Grafe, T. H., Shao, S., et al. 2021. Characterization and mitigation of aerosols and spatters from ultrasonic scalers. *Journal of the American Dental Association*, 152: 981–990.
- Pasquarella, C., Veronesi, L., Napoli, C., Castiglia, P., Liguori, G., Rizzetto, R., Torre, I., Righi, E., Farruggia, P., Tesauro, M., et al. 2012. Microbial environmental contamination in Italian dental clinics: A multicenter study yielding recommendations for standardized sampling methods and threshold values. *Science of the Total Environment*, 420: 289–299.
- Petti, S. 2016. Tuberculosis: Occupational risk among dental healthcare workers and risk for infection among dental patients. A meta-narrative review. *Journal of Dentistry*, 49: 1–8.
- Polednik, B. 2021. Exposure of staff to aerosols and bioaerosols in a dental office. *Building and Environment*, 187: 107388.
- Pourfattah, F., Wang, L. P., Deng, W., Ma, Y. F., Hu, L., Yang, B. 2021. Challenges in simulating and modeling the airborne virus transmission: A state-of-the-art review. *Physics of Fluids*, 33: 101302.
- Remington, D. W., Ott, B. C., Hartka, T. R. 2022. Effectiveness of barrier devices, high-volume evacuators, and extraoral suction devices on reducing dental aerosols for the dental operator: A pilot study. *Journal of the American Dental Association*, 153: 309–318.
- Sergis, A., Wade, W. G., Gallagher, J. E., Morrell, A. P., Patel, S., Dickinson, C. M., Nizarali, N., Whaites, E., Johnson, J., Addison, O., et al. 2021. Mechanisms of atomization from rotary dental instruments and its mitigation. *Journal of Dental Research*, 100: 261–267.
- Sotiriou, M., Ferguson, S. F., Davey, M., Wolfson, J. M., Demokritou, P., Lawrence, J., Sax, S. N., Koutrakis, P. 2008. Measurement of particle concentrations in a dental office. *Environmental Monitoring and Assessment*, 137: 351–361.
- Timmerman, M. F., Menso, L., Steinfort, J., van Winkelhoff, A. J., van der Weijden, G. A. 2004. Atmospheric contamination during ultrasonic scaling. *Journal of Clinical Periodontology*, 31: 458–462.
- To, K. K. W., Tsang, O. T. Y., Yip, C. C. Y., Chan, K. H., Wu, T. C., Chan, J. M. C., Leung, W. S., Chik, T. S. H., Choi, C. Y. C., Kandamby, D. H., et al. 2020. Consistent detection of 2019 novel coronavirus in saliva. *Clinical Infectious Diseases*, 71: 841–843.
- Vernon, J. J., Black, E. V. I., Dennis, T., Devine, D. A., Fletcher, L., Wood, D. J., Nattress, B. R. 2021. Dental mitigation strategies to reduce aerosolization of SARS-CoV-2. *Journal of Dental Research*, 100: 1461–1467.
- Ye, M. J., Sharma, D., Campiti, V. J., Rubel, K. E., Burgin, S. J., Illing, E. A., Ting, J. Y., Park, J. H., Johnson, J. D., Vernon, D. J., et al. 2021. Aerosol and droplet generation from mandible and midface fixation: Surgical risk in the pandemic era. *American Journal of Otolaryngology*, 42: 102829.
- Zhang, M. 2021. Estimation of differential occupational risk of COVID-19 by comparing risk factors with case data by occupational group. *American Journal of Industrial Medicine*, 64: 39–47.